RSC Advances

This is an *Accepted Manuscript*, which has been through the Royal Society of Chemistry peer review process and has been accepted for publication.

Accepted Manuscripts are published online shortly after acceptance, before technical editing, formatting and proof reading. Using this free service, authors can make their results available to the community, in citable form, before we publish the edited article. This *Accepted Manuscript* will be replaced by the edited, formatted and paginated article as soon as this is available.

You can find more information about *Accepted Manuscripts* in the Information for Authors.

Please note that technical editing may introduce minor changes to the text and/or graphics, which may alter content. The journal's standard Terms & Conditions and the Ethical guidelines still apply. In no event shall the Royal Society of Chemistry be held responsible for any errors or omissions in this *Accepted Manuscript* or any consequences arising from the use of any information it contains.

ROYAL SOCIETY OF CHEMISTRY

www.rsc.org/advances

Evaluation of Quercetin-Gadolinium Complex as an Efficient Positive Contrast Enhancer for Magnetic Resonance Imaging†

Thenmozhi Muthurajan, Pooja Rammanohar, Nisha Palanisamy Rajendran, Swaminathan Sethuraman and Uma Maheswari Krishnan*

Centre for Nanotechnology & Advanced Biomaterials
School of Chemical & Biotechnology
SASTRA University, Thanjavur- 613 401, India

*Corresponding Author

Prof. Uma Maheswari Krishnan Ph. D.
Deakin Indo–Australia Chair Professor
Associate Dean for the Departments of Chemistry, Bioengineering & Pharmacy
Centre for Nanotechnology & Advanced Biomaterials (CeNTAB)
School of Chemical & Biotechnology
SASTRA University, Thanjavur – 613 401
TamilNadu,
India

Ph.: (+91) 4362 264101 Ext: 3677

Fax: (+91) 4362 264120

E–mail: umakrishnan@sastra.edu

†Electronic supplementary information (ESI) available.

RSC Advances Accepted Manuscript

Abstract

The need for a highly effective contrast agent that aids in distinguishing normal and affected cells is in great demand in clinics for accurate diagnosis. In this context, the present study attempts to utilize the metal ion complexation capacity of a pharmacologically relevant dietary flavonol, quercetin for development of a novel MRI contrast agent. The flavonoid-metal complex was synthesized using quercetin dihydrate and gadolinium acetate and characterized by elemental analysis, spectroscopy techniques, thermal analysis and powder XRD. The quercetin: gadolinium stoichiometry was determined to be 1:1 using Job's Plot analysis and the equilibrium stability constant of metal binding to quercetin determined from fluorimetric analysis using Stern-Volmer equations indicated excellent stability. The magnetic properties of the complex were typical of a paramagnetic material as confirmed using vibrating sample magnetometry. The antioxidant property of the quercetin-gadolinium complex was greater than that of its parent ligand when evaluated by DPPH assay due to the structural changes. Cyclic voltammetry studies of both quercetin and its gadolinium complex was performed to confirm complexation and its anti-oxidant potential. The viability of cancer cells, MCF7 and normal L929 cells remained unaffected after exposure to the complex. The efficacy of this complex as a positive contrast agent in MRI was evaluated using Phantom agar gel assay and *in vitro* studies. It was found to exhibit superior positive contrast when compared with the commercially available contrast agent. This complex therefore may be evaluated further as a novel MR contrast agent for pre-clinical and clinical applications.

Keywords: Flavonoids, Quercetin, Gadolinium, Stoichiometry, Paramagnetic, MRI, *In vitro*.

Introduction

Flavonoids are polyphenolic compounds that are prevalent in plants including vegetables and fruits which constitute an integral part of diet taken by human beings [1]. It is estimated that

RSC Advances Accepted Manuscript

about 1g of flavonoids is included in a normal human diet per day [2]. Flavonoids are habitually referred to as vitamin P and they are also found to augment the function of vitamin C by improving its absorption and protecting it from getting oxidized [3]. Flavonoids possess diverse biochemical and pharmacological properties including anti-viral, anti-bacterial, anti-allergic, anti-inflammatory, anti-mutagenic, anti-carcinogenic, anti-neoplastic, anti-thrombotic, vasodilator activity scavenging and antioxidant activities constructive to human health [4]. Flavonoids possess the fundamental structure of 2-phenylbenzo-γ-pyrones [5]. Versatile structural variations in the aromatic rings result in different types of flavonoids. Reactive oxygen species are found to cause oxidative damage to biomolecules and organelles leading to many diseases including cancer, Parkinson's disease, asthma, neurodegenerative diseases etc. [6]. Flavonoids possess strong anti-oxidant activity and have been found to be therapeutically beneficial in diseases such as cancer and heart diseases [7]. Quercetin (Q) (3,3',4',5,7-pentahydroxyflavone), a flavonol, is present in the edible portion in majority of dietary plants (e.g., leafy vegetables, roots and tubers, herbs and spices, tea, and cocoa) and has attracted the attention of numerous investigators because of its beneficial biological properties.

Quercetin is a powerful antioxidant that retards oxidation of low-density lipoproteins *in vitro* thereby reducing reactive oxygen species and lipid peroxidation [8, 9]. Quercetin is also found to cause cell cycle arrest of gastric cancer cells and human leukemic T cells in late G_1 phase[10]. More recently, quercetin has been reported to involve in a pathway consisting of heat shock proteins to induce apoptosis in colorectal tumour cells and in HPB-ALL cell line. Quercetin can also down-regulate p53 levels and it is also a potent inhibitor of important enzymes in pathways involving signals for proliferation [11]. Quercetin was the first tyrosine kinase inhibitor to be investigated [12]. Hence, use of quercetin or its derivatives for diverse applications is an area of active research across the globe.

RSC Advances Accepted Manuscript

The complexation of metal ions by flavonoids plays a central role in limiting bioavailability of metal ions and suppressing their toxicity. The antioxidant property of flavonoids has also been attributed to its ability to complex with metal ions and scavenges free radicals. The process of chelation occurs by carbonyl and hydroxyl groups present in flavonoid molecules. Quercetin also serves as a bidentate ligand towards rare earth metal (III) ions and might form a mononuclear complex with one ion bonded to three ligands [13]. Quercetin possesses three possible chelating sites: the 3-OH and carbonyl, the 5-OH and carbonyl, and finally the 3' and 4'- catechol moiety (Figure S1, ESI†) [14]. Rare earth metal (III) complexes with quercetin can bind to DNA thereby altering its transcription and repressing the growth of tumour cells [15]. Aluminium has been implicated in neurological and bone disorder and the complexation of Al (III) by quercetin reduces aluminium overload in the diet [16]. The complexes of Gd(III) and Eu(III) ions with quercetin show antioxidant and therapeutic (blood cancer) properties. Most of the reports on quercetin-metal ion complexes have focused only on their anti-microbial and anti-cancer effects and other applications, especially in the field of diagnostics, remain to be investigated.

Gadolinium (Gd) a lanthanide element, is popular in medical diagnostics [17]. The unique magnetic properties of gadolinium (III) ion have been exploited in medicine for magnetic resonance imaging (MRI). Gadolinium (III) is highly preferred as it has 7 unpaired electrons. Gadolinium (III) chelates like $[Gd(DTPA)(H_2O)]^{2-}$ have been successfully used in radiologic practice and also in medicine [17]. As Magnetic Resonance Imaging (MRI) is relied upon by different specialties, gadolinium is being widely employed by ophthalmologists, cardiologists, urologists, neurologists, and others to visualize functional changes in the body. Over the last few decades, significant efforts have been made to improve contrast of MRI using contrast enhancing agents. The MRI contrast agents can be broadly classified as negative and positive contrast agents. The complexes of gadolinium (III) are commonly used

RSC Advances Accepted Manuscript

in clinical MRI applications to enhance contrast by selectively inducing relaxation of water molecules in the vicinity of the complex and are categorized as positive contrast agents. In order to identify molecular targets, it is essential to improve the sensitivity (relaxivity) of these contrast agents [18]. However, such chelates have also been associated with adverse effects leading to severe conditions such as Nephrogenic Systemic Fibrosis [19]. Signal intensity in MRI systems varies significantly from 1/T1, the longitudinal relaxation rate of protons from water, and the transverse relaxation rate, 1/T2. The signal tends to decrease with increasing 1/T2 and increases with increasing 1/T1. Because of toxicity associated with unaltered gadolinium ions, it is complexed with an appropriate ligand to create a clinically useful and safe intravenous MRI contrast agent. Complexation prevents the binding of Gd(III) ions to donor groups in proteins and enzymes [20]. Gadolinium forms stable chelates with ethylenediaminetetraacetic acid (EDTA) and diethylenetriamine pentaacetic acid (DTPA). Chelation of gadolinium (Gd) with DTPA results in the formation of a strong paramagnetic complex. The combination of rapid urinary excretion, strong proton relaxation, and high tolerance favours the use of gadolinium-DTPA in clinics as a positive contrast enhancer in magnetic resonance imaging [21]. However, gadolinium complexes have been recently identified to be associated with renal toxicity owing to transmetallation and ligand exchange reactions [22]. Hence, safe alternate needs to be designed for contrast enhancement applications in MRI. Gadolinium-based inorganic nanoparticles and nanostructured manganese oxides have emerged as new types of positive (T1) MRI contrast agents exploiting the high surface concentration of metal ions possessing high magnetic moments. These nanostructured T1 contrast agents have been functionalized and used for multimodal imaging, targeted imaging, and to simultaneously image and deliver drugs [20]. Long term toxicity evaluation of these molecules need to be carried out to establish their usefulness. The scan of literature reveals that the field for development of novel contrast

RSC Advances Accepted Manuscript

enhancing agents remains wide open. The present work attempts to synthesize and characterize a quercetin-gadolinium (QGd) complex and evaluate its potential as a novel positive contrast agent for MRI applications – a facet that has never been explored earlier.

Materials and Methods

Materials used

Quercetin dihydrate (97%, Alfa Aesar, England) and gadolinium (III) acetate hydrate (99.9%, Alfa Aesar, England) were used as such for the synthesis of the complex without any further purification. Methanol (Merck, India) and dimethyl sulfoxide (DMSO, Merck, Germany) were used as solvents for synthesis. 1,1- Diphenyl-2-picrylhydrazyl (DPPH) radical (Sigma Aldrich, USA) was used for the anti-oxidant assay. For synthesis and other experiments, nitrogen purged Milli-Q water was used. Cell culture and cell viability studies were performed using MCF7 breast cancer cell line, L929 murine fibroblast cell line (NCCS, Pune), Dulbecco's Modified Eagle Medium, 5% fetal bovine serum (Gibco, NZ), 1% penicillin G, and streptomycin (Gibco, NZ), 96 well plates and MTS assay kit (CellTiter 96 Aqueous one solution, Promega, USA).

Synthesis of Quercetin- Gadolinium(III) complex

Quercetin dihydrate (0.1M) was dissolved in 25 mL of methanol and 0.1M of NaOH was added to the solution. Then, gadolinium(III) acetate hydrate (0.1M) dissolved in 25 mL of methanol was added slowly. The reaction mixture was stirred at room temperature for about 6 h and the solvent was then evaporated. The sample was collected, washed with 1:1 chloroform/n-butanol and water to remove the unreacted molecules. The samples were dried in vacuum and the yield of quercetin-gadolinium (QGd) complex was found to be 52.57%.

Characterization of QGd complex

RSC Advances Accepted Manuscript

The QGd complex was characterized by means of the following techniques. The elements, carbon and hydrogen of the complex were analysed using Perkin-Elmer 2400 Series CHNS analyser. The UV Visible spectrum of the QGd complex in DMSO solvent was recorded at room temperature (RT) using double beam UV-Visible spectrophotometer (Lambda 25, Perkin-Elmer, USA). The binding of flavonol Q and metal-ion Gd was studied using FT-IR spectroscopy (Spectrum100, Perkin Elmer, USA) in the range of 400– 4000-cm^{-1} using KBr pellets. The band gap of the complex was studied using photoluminescence spectra, obtained using Perkin Elmer LS 50B photoluminescence spectrometer. The thermal properties of the complex was studied using thermogravimetry (TG-DTA, SDT-Q600, TA instruments, USA), from 28°C to 1000°C at a rate of 10°C/min and differential scanning calorimetry (DSC, Q20-DSC, TA instruments, USA). Electron Spin Resonance (ESR) spectrum for the complex was recorded using JEOL Model JES FA200, Japan, at X band frequency. The elemental composition and purity of the complex was measured using X-ray Photoelectron spectroscopy (K-Alpha, Thermo Scientific, UK). The survey scan was performed in the range of 0-1350eV.

The stoichiometry and the binding constant of the complex were found using UV-visible spectrophotometry (Lambda 25, Perkin Elmer, USA) at an absorption wavelength of 461 nm and fluorescence spectrometry (LS45, Perkin Elmer, USA) using excitation and emission wavelengths of 454 nm and 504 nm respectively. A stock solution of ligand (quercetin dihydrate) and metal (gadolinium (III) acetate hydrate) of 10mM concentration was prepared in DMSO. Solutions of different volumetric ratios were added and absorbance was measured spectrophotometrically. The metal to ligand ratio of the metal-ligand interaction was ascertained using mole-ratio plots and was further confirmed by the Jobs' continuous variation method. In the case of mole-ratio method, a series of solutions were prepared by maintaining the concentration of ligand and gradually varying the concentration of metal ions

RSC Advances Accepted Manuscript

and vice-versa. The solutions were mixed well to attain equilibrium between ligand and metal ions and the optical spectrum of each solution was then recorded. The optical density (OD) values obtained were then plotted against ratio of concentration of gadolinium (III) to quercetin, *i.e.*, C_M/C_L where C_M and C_L are the concentrations of the metal ion (Gd) and the ligand (Q) respectively. The metal to ligand ratio (M/L) at which maximum binding occurs was then obtained. Job's method of continuous variation, in which, a series of solutions with different ligand and metal ion concentrations were prepared by maintaining the total ligand and metal ion concentration (C), constant [*i.e.,* $C = C_M+C_L$ where C, C_M and C_L are the total concentration of metal ion (Gd) and ligand (Q), the concentration of the metal ion (Gd) and the concentration of the ligand (Q) respectively].

The X-ray diffraction pattern of the powder QGd sample was recorded using Bruker D8 X-ray diffractometer, Germany with Cu-Kα radiation to determine its crystalline nature. Lakeshore VSM 7410 vibrating sample magnetometer was used to determine the magnetic properties of the samples at room temperature. The cyclic voltammetry (CV) experiment was performed using electrochemical workstation (CH603C CH Instruments, Austin, TX) for studying the electrochemical property of the QGd complex. A conventional three electrode system was used to record the cyclic voltammograms of quercetin and its complex with gadolinium (III). Glassy carbon, platinum and Ag/AgCl electrodes were used as working, reference and standard electrodes, respectively. For analysis, 1mM solution of Quercetin and Quercetin-Gadolnium complex was prepared in DMSO. The electrochemical study of the flavonoid and its metal complex was done using equimolar amount of tetra-n-butyl ammonium perchlorate (TBAP) as a supporting electrolyte. The samples were scanned in the range of +1.00V to -1.25V at the scan rate of $100mVs^{-1}$ and at 1mV interval.

The anti-oxidant property of the compounds was determined employing UV-Vis spectrophotometry for carrying out DPPH assay. A solution of DPPH (0.1mM) was prepared

RSC Advances Accepted Manuscript

by dissolving it in DMSO and maintained in dark. The stock solutions of quercetin dihydrate(1mM) and quercetin-gadolinium complex(1mM) were also prepared in DMSO. Different concentrations of quercetin dihydrate and quercetin-gadolinium complex (5, 10, 15, 20, 25, 30, 35, 40, 45, 50, 100, 200 and 500 µg/mL) dissolved in DMSO were added to 3mL of DPPH solution and the reaction mixture was shaken vigorously. The reduction in absorbance of DPPH was followed at 520 nm. As a control, the absorbance of blank DPPH solution before the sample addition was recorded at 520nm. Further the percentage radical scavenging activity was calculated using the formula, $\%RSA= ((A_c-A_s)/A_c)*100$, where A_c is the absorbance of control, A_s is the absorbance recorded after addition of sample.

Cell culture and cell viability

Cell culture and cell viability of quercetin (Q) and quercetin-gadolinium (QGd) complex were carried out in a 5% CO_2 environment and 37^oC in an incubator (Autoflow 8700, Nuaire, USA) to maintain adequate environment for cell growth. Stock solutions of Q and QGd complex were prepared in 0.1% DMSO and diluted to the required concentration during the cell culture. MCF7 breast cancer cells and L929 fibroblast cells were cultured in DMEM medium supplemented with 10% FBS and 5% P/S at 37°C in a 5% CO_2 incubator. The medium was changed on every alternate day, until the cells became confluent. A breast cancer cell line and a normal fibroblast cell line were chosen to toxicity of Q and QGd in cancer and normal cells. The toxicity of the compounds Q and QGd was determined by MTS assay separately in MCF7 (breast cancer cells) and L929 (normal fibroblasts) after 24h and 48h of culture. About 10,000 cells/well were seeded in a 96-well plate and allowed to adhere for 24h. Samples at 1, 10, 50, 100 and 200 µg/mL concentrations were added and further incubated for 24h and 48h. After the prescribed time, cell viability was evaluated by addition of MTS reagent and measuring the absorbance of the samples. TECAN infinite M 200

RSC Advances Accepted Manuscript

multimode reader (Switzerland) was used to measure the absorbance changes on addition of MTS reagent.

Phantom agar gel assay sample preparation

A phantom consisting of a set of 15 mL tubes filled with samples having concentrations of 0, 10, 50, 100, 200 and 500µg/mL of gadolinium (III) acetate salt and quercetin-gadolinum complex was prepared in 9 mL Phosphate Buffered Saline (PBS) solution. In each tube, the sample was preheated to 60°C (to avoid solidification of the gel) and then mixed with 1mL of 5% agarose solution prepared in PBS to make up a final volume of 10 mL. After this, the setup was cooled at room temperature to form the gel. The magnetic resonance imaging studies were done using a 1.5 T scanner (Brivo MR355 1.5T, GE Health care, USA). The phantom containing agar gels were situated at iso-centre of the magnet and T1 and T2 weighted images were achieved in the coronal section. T1 calculations were done from the images acquired with a spin-echo pulse sequence by means of the subsequent parameters such as, a slice thickness of 4mm with a constant TE of 20 ms and with variable TR (repetition time) of 100, 200, 300, 500, 600, 800, 1000, 1500, 2000, 3000, 4000 and 5000 ms. Using the spin-echo sequence the T2 relaxation was calculated using a fixed TR of 5000ms with variable TE of 20, 40, 60, 80, 100, 120, 140, 160, 180, 200, 220, 240, 260, 280, 300, 320ms and the slice thickness was retained as 4mm. From the MR signal intensity data obtained for different concentrations of gadolinium acetate, quercetin-gadolinium complex and gadopentetate dimeglumine, the transverse relaxation rates R_1 and R_2 were calculated by mono-exponential curve fitting using the equations for relaxation rate R_1: $y = A \times [(1-\exp(-R1xTR)]$ and for relaxation rate R_2: $y = A + C [\exp(-R_2xTE)]$, where TR denotes recovery time and TE denotes echo time. The relaxivity values r_1 and r_2 were calculated using the standard equation $R_i = Ri_0 + [Gd^{3+}] \times r_i$.

RSC Advances Accepted Manuscript

***In vitro* MRI studies**

About $5x10^4$ MCF7 and L929 cells per well were seeded in six well plate and allowed to grow for 24 h. After 24 h the cells were incubated with Quercetin-gadolinium complex at different concentrations ranging from 1 to 200µg/mL dispersed in medium. After 3 h, 8 h and 24 h the cells were collected in 15mL polypropylene tubes and centrifuged at 3000 rpm for 5 minutes. The pellet was re-dispersed and washed twice with PBS and the cells were then dispersed in 3 mL of 5% agarose and allowed to solidify. Finally the tubes were sealed with 5% agarose to prevent evaporation of water. The samples were then placed in the MRI system and T1 and T2 were recorded.

Results and discussion

Characterization of Q and QGd complex

Physicochemical properties: The synthesized quercetin-gadolinium (QGd) complex was brownish green in colour and was stable at room temperature. The QGd complex was found to be soluble in DMSO and DMF but is sparingly soluble in methanol, ethanol, acetone, diethyl ether, chloroform and insoluble in water, n-hexane, and DCM solvents. The binding energy of quercetin-gadolinium (QGd) complex obtained using photoluminescence spectroscopy was found to be 3.06eV, which is lesser than the binding energy obtained for quercetin (3.19eV). This shift may be attributed to the complexation of quercetin with gadolinium resulting in the reduced binding energy[23].

Elemental analysis: Calculation of carbon and hydrogen content of quercetin and its complex with gadolinium (III) metal ion was performed assuming a metal: ligand:H_2O ratio of 1:1:2. The calculated values (%) for QGd were: C 26.75 and H 2.08 while the experimental values were: C 21.49 and H 2.93. The good agreement of the experimental values obtained with the calculated values suggests that the QGd complex has a metal:ligand:H_2O ratio of 1:1:2.

RSC Advances Accepted Manuscript

UV-Vis spectrophotometry: Most flavones and flavonols like quercetin exhibit two major absorption bands in the UV-Vis region [13] namely band I in the range 300-500 nm corresponding to the absorption of the cinnamoyl system related to the conjugated system between carbonyl of ring C and ring B (Figure S1, ESI†). Band II in the range 200-280 nm corresponding to the benzoyl system due to the conjugated system between ring A and carbonyl ring of C, related to the n-π* and π- π * transitions [4, 24]. In the present study, quercetin exhibits a strong and large absorption band with maximum at 371.8 nm due to band I while band II appears at 254.2 nm (Figure S2A, ESI†). The UV-Vis spectrum of the QGd complex shows a pronounced bathochromic shift to 461 nm (band I)and the strong absorption corresponding to band II appears at 293 nm in the spectrum. The bathochromic shift observed for the metal complex supports the coordination of quercetin to metal possibly through 4-oxo-5-hydroxyl moieties. A weak transition is observed for QGd around 14065 cm^{-1} (inset of Figure S2A, ESI†) which may be attributed to the f-f charge transfer bands corresponding to $^2T_{2g} \rightarrow {}^2E_g$ transition [25].

FTIR spectroscopy: The FTIR spectrum of the Quercetin (Q) and Quercetin-Gadolinium complex (QGd) is shown in Figure S2B, ESI†. The comparison of the spectra of the ligand, quercetin with quercetin-Gd(III) ion complex is shown in Table 1. Bands at 553–465 cm^{-1} are due to the presence of *v* (Gd-O) stretching vibrations, indicating the formation of metal complex, whereas these bands were absent in the FTIR spectrum of the ligand quercetin [26]. The *v*(C-O-C) frequency and v_{ring}(C=O) (ie., C ring, Figure S1, ESI†) frequencies exhibit a shift towards the lower energy. A similar shift towards the lower energy is also observed in the *v*(C-OH) frequency suggesting that the complexation involved the C=O and C-OH moieties.

RSC Advances Accepted Manuscript

Table 1. FTIR spectrum of Quercetin and Quercetin-gadolinium complex

Compound	*ν*(O-H)	*ν*(C=O)	*ν* (C=C)	*ν* (C-OH)	*ν* (C-O-C)
Q	3409-3144	1665.50	1611.86	1382.87	1262
QGd	3437–3128	1648.36	1607.68	1363.57	1250

Thermal studies of Q and QGd complex

Heating of a material causes chemical and physicochemical alterations, which are supplemented by the absorption or liberation of heat [27]. Thermal behaviour of quercetin and quercetin-gadolinium complex was investigated using differential scanning calorimetry (DSC) and thermogravimetric analysis (TGA) (Figure 1A). The TG-DTA results show that quercetin and its gadolinium complex undergo three distinct decompositions between 0 and 1000^{o}C. An initial weight loss of about 11% was observed around 110^{o}C for both quercetin and QGd complex owing to the removal of free water molecules. The QGd exhibits an intermediate weight loss between 140-190^{o}C that is absent in the TG of quercetin. The heat flow measurements of QGd reveal that this weight loss corresponds to an endothermic peak at 165^{o}C which may be due to removal of coordinated water molecules (Figure 1B)[28, 29]. The weight loss corresponding to the loss of coordinated water molecules was found to be 5% which correlates with the loss of two water molecules. This finding is in agreement with the elemental analysis results which suggested a metal:ligand:H_2O ratio of 1:1:2 for QGd. Both quercetin and QGd exhibit further weight loss between 285 to 560^{o}C and between 280 to 525^{o}C respectively which may be attributed to the degradation of the aromatic rings of the ligand. While quercetin exhibits nearly total weight loss by 560^{o}C, the QGd complex was found to leave a residue of 32% confirming the presence of the inorganic gadolinium in the complex. The thermograms of quercetin and its gadolinium complex show endothermic peaks in agreement with mass changes (Figure 1B). The first endothermic peak observed in the

RSC Advances Accepted Manuscript

thermogram at 115°C and 125°C for QGd complex and Q respectively shows corresponds to the mass loss which due to elimination of water molecules. The second endothermic peak in the region of 165°C for QGd corresponds to the removal of coordinated water molecules which is absent in the thermogram of quercetin. Quercetin exhibits a sharp endothermic peak at 324°C corresponding to its melting point while the melting point of QGd is shifted to a higher temperature (520°C) confirming the complexation of Gd with quercetin. An exothermic peak is observed for quercetin at 353°C, indicating the onset of sample decomposition [30].

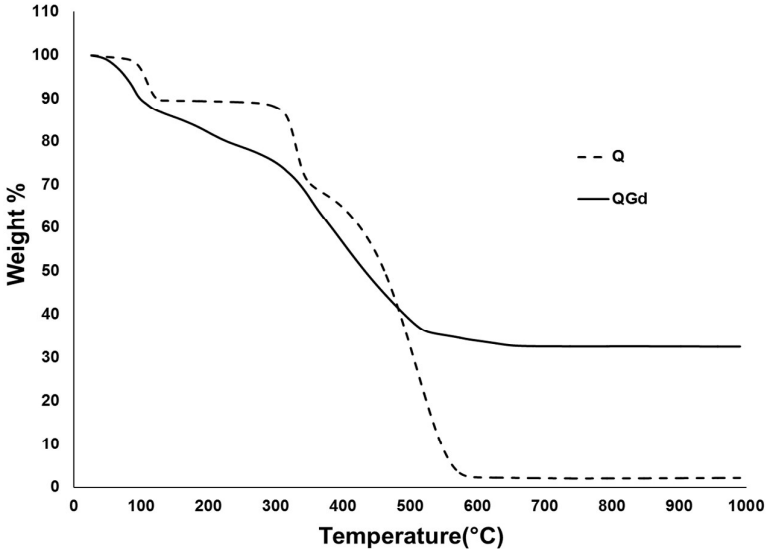

Figure 1A. TG spectrum of quercetin and quercetin-gadolinium complex

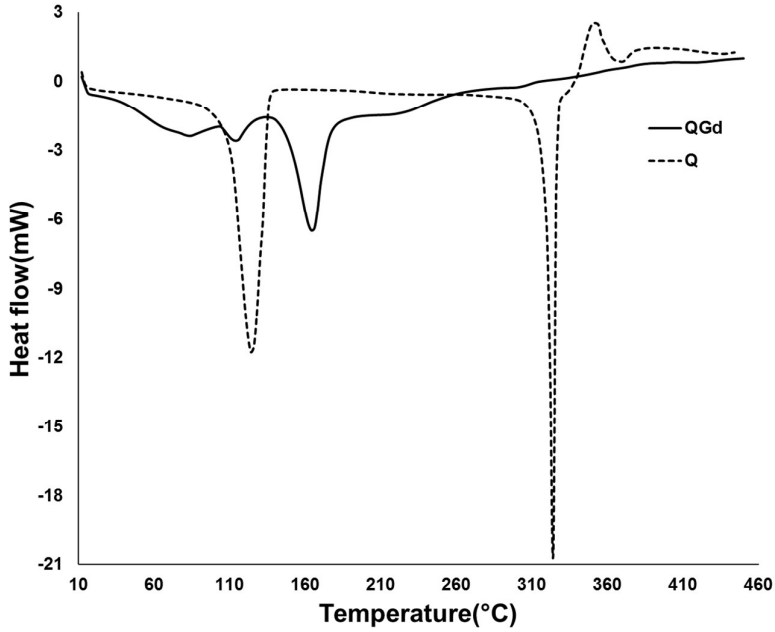

Figure 1B. DSC spectrum of quercetin and quercetin-gadolinium complex

RSC Advances Accepted Manuscript

Electron paramagnetic resonance studies of QGd complex

In general, the EPR spectrums of most paramagnetic compounds are recorded in the frequency range of 9-10 GHz [31]. The EPR spectrum of QGd complex at room temperature contains a broad band with no hyperfine splitting (Figure S3, ESI†). The g-values obtained for QGd complex were g_x= 2.3051, g_y= 2.0132 and g_z = 1.6617, respectively, where $g_x \neq g_y \neq g_z$. From the values of g tensors it may be inferred that the QGd complex could adopt monoclinic ESR symmetry. As the g values of QGd are not identical to that of free electron (g = 2.0023) it may be concluded that it does not exist in the semiquinone form [32, 33]. The broad band indicates that the dipolar interaction of Gd (III) is small. The g value of an isolated gadolinium (III) ion is normally below g < 2, but in the powder or bulk state, the g value is > 2 [34]. The main part of the EPR spectrum arises from the high spin state (S=7/2) of gadolinium (III) ions. Because of its $^8S_{7/2}$ ground state and the exicited state making a small orbital contribution, it can show static and dynamic interaction with its host system [35].

X-ray Photoelectron Spectroscopy studies of QGd complex

The elemental analysis and binding energy of the elements in gadolinium acetate and quercetin-gadolinium complex were studied using X-ray Photoelectron Spectroscopy (XPS) (Figures 2A and 2B). The C(1s) spectrum shows the typical peaks for C-C, C-O-C and O-C=O components. The C(1s) spectrum of gadolinium acetate consists of a peak at 290.78 eV due to C=O bond and two other peaks at 294.58 eV and 285.68 eV respectively, which may be attributed to acetate and C-O-C functional groups, respectively on the surface of the sample (Figure 2A). In the case of QGd complex, two peaks were obtained at 289.28 eV and 286.48 eV due to O-C=O and C-O-C respectively (Figure 2B). The carbonyl peak at 290.78 eV in gadolinium acetate exhibits a negative shift towards lower binding energy to 289.28 eV in QGd suggesting the involvement of O-C=O in the formation of the complex.

RSC Advances Accepted Manuscript

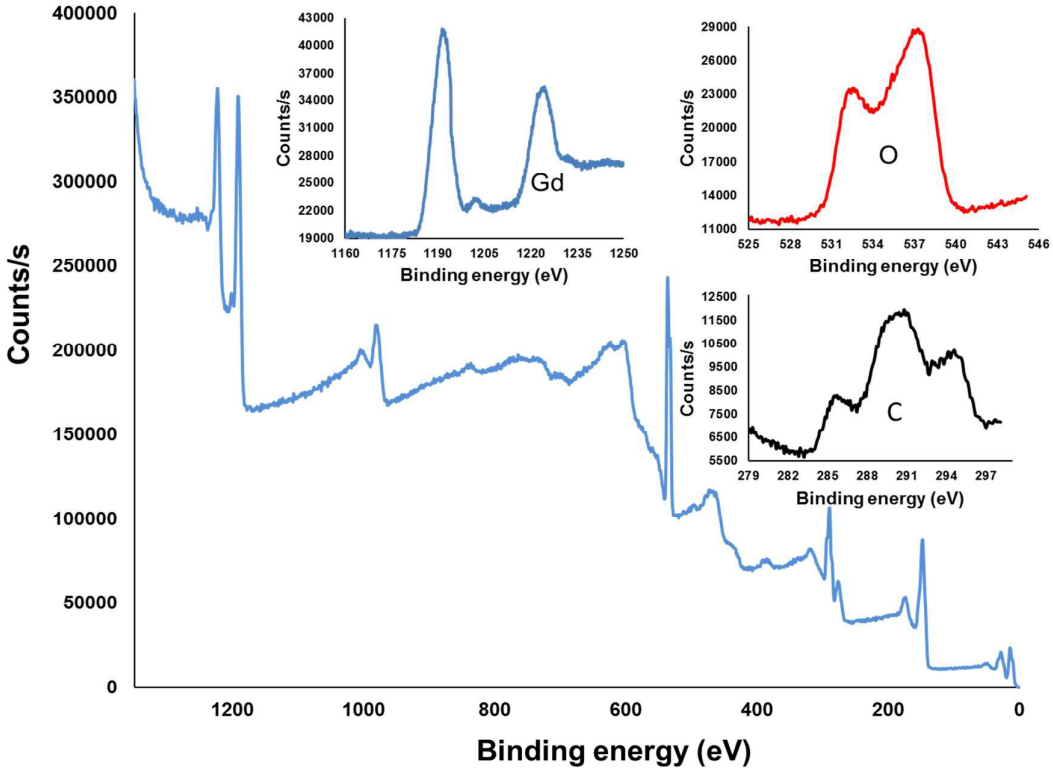

Figure 2A. XPS spectrum for gadolinium acetate

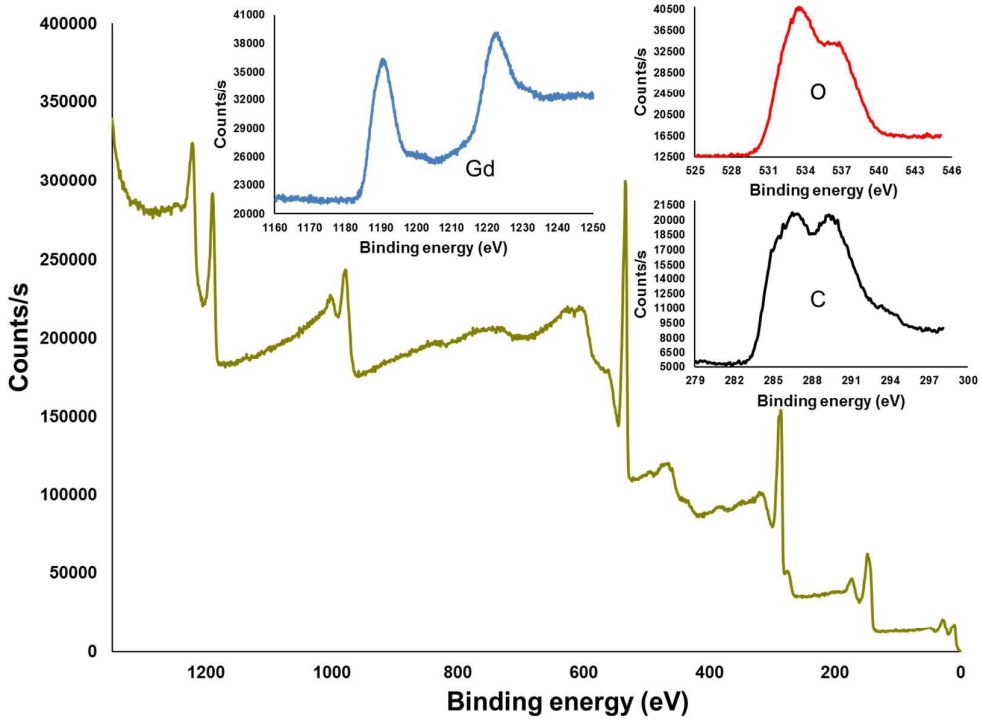

Figure 2B. XPS spectrum for quercetin-gadolinium(III)

RSC Advances Accepted Manuscript

The O(1s) spectrum of gadolinium acetate is dominated by peaks at 537.28 eV and 532.58 eV and QGd complex exhibits peaks at 533.48 eV and 536.78 eV. The slight shift in the peaks suggests the involvement of organic C=O (~ 533 eV) in the complexation [36]. The Gd (3d) spectrum of gadolinium acetate had two notable peaks at 1224.38 eV and 1191.28 eV respectively which are shifted to 1222.98 eV and 1190.38 eV respectively in the quercetin-gadolinium complex. The peak positions are in good agreement with the Gd(3d) level consisting a spin orbit split, at 1186.74 eV, reported in literature [37]. The 4d spectrum of gadolinium acetate exhibited a peak at 148 eV which shifted to 147 eV in QGd complex. The reduced binding energies encountered in both 3d and 4d spectrum of QGd suggests its involvement in complex formation.

Determination of stoichiometry and stability constant of QGd complex

Job's plot: A spectroscopic analysis of interaction between the flavonoid quercetin and gadolinium (III) ions was carried out using Job's method of analysis. Figures S4A and S4B, ESI† depict the Job's plot obtained using the mole-ratio and continuous variation methods. From the absorbance values obtained in the mole-ratio method, the metal to ligand ratio was found to be 1:1 for formation of QGd (Figure S4A, ESI†). This result was further confirmed by Job's method of continuous variation (Figure S4B, ESI†). The plot of absorbance versus (C_L/C_L+C_M) gives a value of 0.5, which implies a 1:1 proportion for ligand to metal ratio[38, 39]. This result is in agreement with the inferences arrived from the elemental analysis.

Determination of stability constant: The fluorescence intensity of a molecule can decrease when it interacts with another molecule. The interactions may be static or dynamic based on molecular rearrangements, collisional quenching, and energy transfer [40]. Such a decrease in the fluorescence intensity on interaction with another molecule is known as fluorescence quenching which is usually described using Stern-Volmer equation [41]. Various volumes of the metal solution (Gd(III)) was added to a known concentration of the ligand quercetin

RSC Advances Accepted Manuscript

resulting in fluorescence quenching. The decrease in fluorescence intensity with subsequent addition of known volume of metal solution at the excitation wavelength (λ_{ex}=454nm; λ_{em}=504nm) was recorded and the values were substituted in the Stern-Volmer equation. The stability constant of the complex can be determined from the slope of the plot of C vs F_o/F_c, where C is the concentration of the ligand, F_o is the initial fluorescence intensity of the ligand without addition of metal and F_c is the fluorescence intensity after addition of known volume of gadolinium acetate (Figure S5, ESI†). From the plot, it was found that the binding constant of the metal to ligand for quercetin-gadolinium(III) was 1.162×10^5 M^{-1} [42, 43]. This value is similar to those reported for quercetin-copper(II)-DNA complex [44].

Powder XRD studies of Q and QGd complex

The X-ray diffractograms of quercetin and its complex with gadolinium were examined in the range of 10–60° at a wavelength of 1.543 Å and the results are presented in Figure 3. The diffractograms and the associated data depict the 2θ value for each peak, the relative intensity and inter-planar spacing (*d*-values) [45]. From the X-ray diffraction pattern of the complex, major peaks of relative intensity greater than 10% was considered for further interpretation [46]. Presence of sharp peaks in the diffractograms of both molecules indicates their crystalline nature. The pure ligand, quercetin, shows a sharp, highly intense peak at 2θ value of 27.25°. Similarly, the QGd complex also exhibits a peak at 27.22° but with lesser intensity. The presence of an intense peak at 25.66° in the complex indicates the complexation of the ligand quercetin with gadolinium (III). The average crystallite size can be determined using Debye Scherrer's formula $D = \kappa\lambda/\beta\cos\theta$, where D is the mean crystallite size, κ is coefficient and is equal to 0.94 here, λ is the wavelength of the X-ray radiation used, β is full width half maximum and θ is the angle from the corrected position [47]. The crystallite size determined using Debye Scherrer's formula for quercetin and QGd were 23.220 nm and

RSC Advances Accepted Manuscript

41.470 nm respectively. The diffraction pattern of the complex was indexed by standard methods and the (h k l) values were calculated using DICVOL91 software [48]. Comparison of the results (Tables 2A & 2B), reveals that there was good agreement between the values of 2θ and d values and it correlates the literature information [49]. Using dichotomy method, the unit cell of reduced volume was obtained and the direct cell parameters of QGd complex were found to be A = 8.9469(0.012)Å, B = 3.7877(0.004)Å, C = 7.646(0.020) Å and β = 104.517(0.100)° corresponding to a monoclinic system. Similar formation of monoclinic systems have been reported in literature for heteronuclear complexes of Ln^{3+}-Fe^{3+} and Ln^{3+}-Co^{3+} complexes (Ln: lanthanide) that were bridged by cyanide moieties [50] and lanthanide complexes with 3-hydroxypicolinic acid [51].

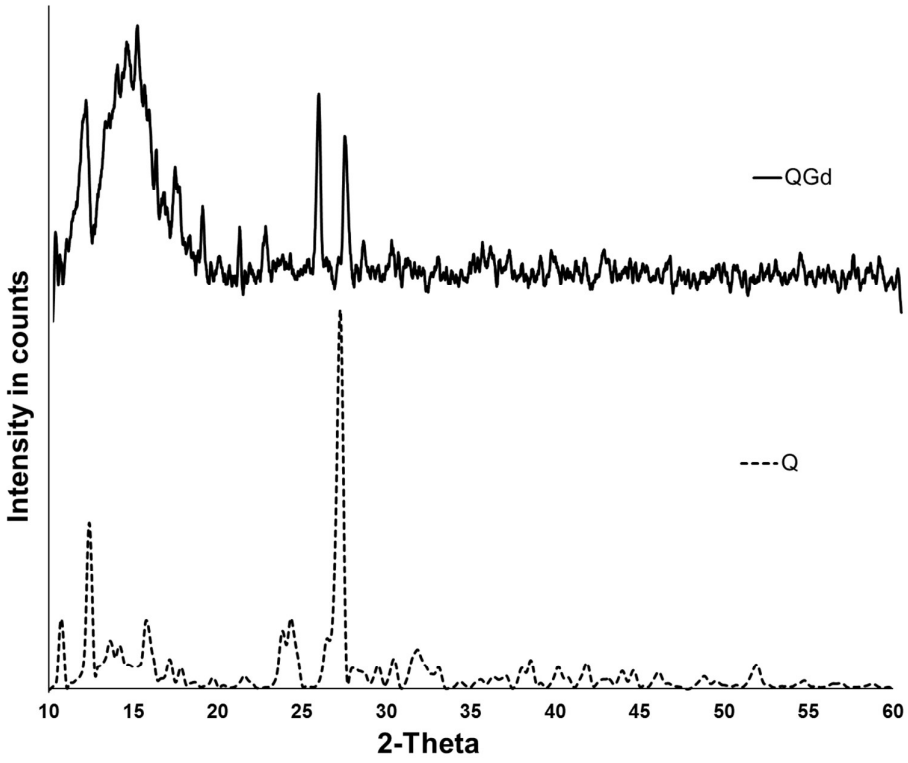

Figure 3. Powder X-ray diffractogram for Q and QGd complex

RSC Advances Accepted Manuscript

Table 2A. Powder X-ray data for quercetin

h	k	l	d Observed	d Calculated	2θ Observed	2θ Calculated
2	0	-1	8.242	8.24614	10.725	10.720
2	0	0	7.141	7.13961	12.385	-12.388
0	0	2	5.615	5.62095	15.770	15.753
3	0	-2	5.167	5.17658	17.147	17.115
2	0	1	4.975	4.97797	17.814	17.804
0	1	0	3.730	3.73082	23.836	23.831
3	0	-4	3.270	3.26519	27.250	-27.291
3	1	-2	3.026	3.02667	29.495	29.488
3	1	0	2.935	2.93630	30.431	30.418
0	0	4	2.809	2.81048	31.832	31.815
4	1	1	2.334	2.33204	38.542	-38.575
5	0	-6	2.156	2.15615	41.867	41.864

Table 2B. Powder X-ray data for quercetin-gadolinium(III) complex

h	k	l	d Observed	d Calculated	2θ Observed	2θ Calculated
1	0	0	8.6911	8.66125	10.17	10.205
0	0	1	7.40296	7.4021	11.945	11.947
2	0	-1	4.22573	4.22833	21.006	20.993
1	1	0	3.46803	3.47036	25.666	25.649
1	1	-1	3.27335	3.27098	27.221	27.242
4	1	2	1.54563	1.5457	59.785	59.782

Vibrating sample magnetometer measurements of QGd complex

The magnetic saturation effects of gadolinium (III) acetate and the quercetin-gadolinium complex were evaluated using vibrating sample magnetometry. Magnetization of quercetin and QGd are shown in Figure 4 and their magnetic moments were analysed. It is known that gadolinium (III) salts are paramagnetic in nature and they therefore, exhibit a linear relationship between magnetic susceptibility and field strength [52]. The saturation magnetization of gadolinium (III) acetate was found to be 0.91443 emu/g and that of quercetin-gadolinium complex was 0.40507emu/g. Interestingly, the hysteresis loop had not opened up for QGd complex. A decrease in the net magnetization of the complex on comparison with that of the pure salt can be attributed to the fact that coordination of the

RSC Advances Accepted Manuscript

flavonoid quercetin with gadolinium (III) in a 1:1 ratio thereby resulting in around 50% reduction in the magnetization. The complex however exhibited paramagnetic behaviour which suggests that it can act as a potent MRI positive contrast agent.

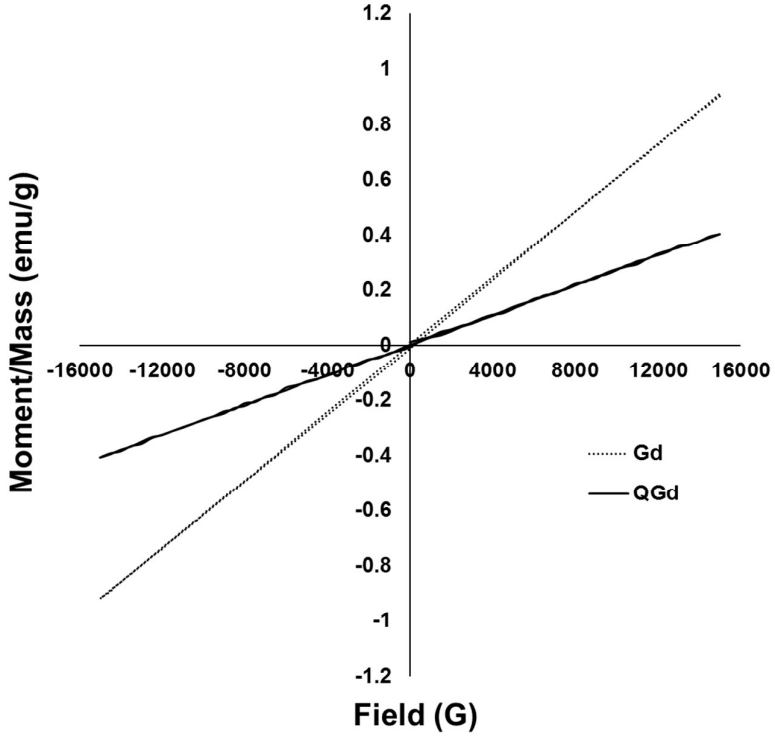

Figure 4. Magnetometry graph for gadolinium acetate hydrate and quercetin-gadolinium (III) complex

Electrochemical analysis of Q and QGd complex

The electroactivity of the complex was investigated using cyclic voltammetry. This technique is usually used to characterize the antioxidant activity of a molecule by estimating its redox potential [53]. The compounds that get oxidized at relatively lower potentials tend to have strong radical scavenging activity. The presence of a number of hydroxyl groups in the structure of flavonoids contribute to their antioxidant activity. Greater the number of hydroxyl or electron donating groups, higher will be the antioxidant activity of the compound [28]. From the cyclic voltammogram of quercetin, it is observed that there is a sharp oxidation peak (1) at a potential of -0.825V and a corresponding current of 1.33×10^{-5} A (Figure 5). The electrochemical oxidation of quercetin has earlier been reported to be a complex process

RSC Advances Accepted Manuscript

dependent on the pH, concentration, supporting electrolyte and scan rate used for the analysis[54]. The appearance of a single oxidation peak in the cyclic voltammogram of quercetin is typical for those reported at higher pH and has been attributed to the formation of an orthoquinone product due to the oxidation of the catechol moiety in ring B of quercetin [54]. Literature reports have indicated that the electron donating hydroxyl groups at positions 5 and 7 of ring A also undergo oxidation but at still higher potentials [55] and this reaction are reversible. A small, but perceptible reduction peak (2) appears at -0.659 V in the cyclic voltammogram of quercetin due to the partial reduction of the catechol moiety and the very small difference in the peaks (ΔE_p = 16.6 mV) is typical of fast electron transfer reactions at the electrode surface. Another small reduction peak (3) is observed at +0.4 V which may be attributed to the reduction of the 5-OH in the ring A of quercetin. The cyclic voltammogram of quercetin-gadolinium (III) complex exhibits a similar profile as the parent ligand with the oxidation peak appearing at -0.824 V but the first reduction peak was shifted to -0.63 V. The higher oxidation current of 1.783×10^{-5} A observed in the cyclic voltammetry suggests that the complexation has enhanced the oxidation tendency of quercetin and consequently it may be inferred that the QGd complex possesses higher antioxidant activity when compared to its parent ligand. Similarly, the reduction current is also higher for the complex when compared to quercetin. Interestingly, the second reduction peak (3) observed in the cyclic voltammogram of quercetin is absent in the voltammogram of QGd. This is because the 5-OH is involved in the complexation with gadolinium and hence is not available for undergoing redox reactions.

RSC Advances Accepted Manuscript

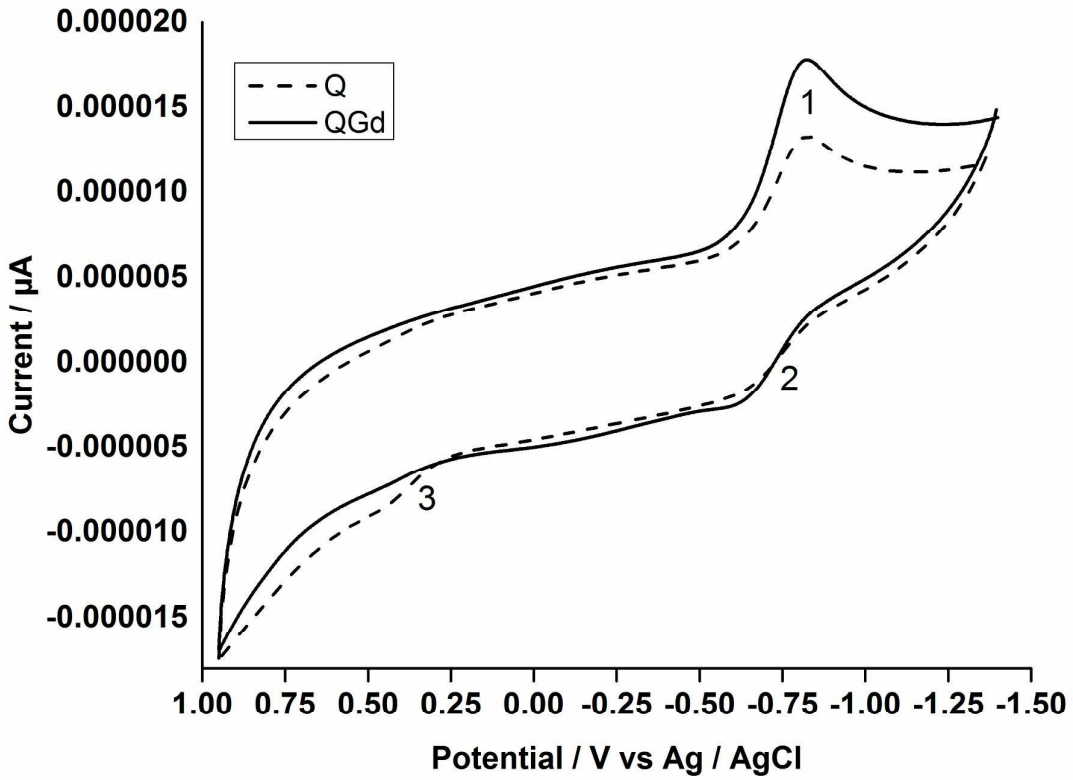

Figure 5. Cyclic voltammograms of quercetin and quercetin-gadolinium (III) complex with Tetra-n-Butyl Ammonium Perchlorate as supporting electrolyte

Scavenging activity on DPPH radical of Q and QGd complex

The antioxidant activity of quercetin and quercetin-gadolinium complex was investigated using DPPH assay by varying the concentrations from 5-500 µg/mL at various time of incubation (Figure 6). The efficiency of the QGd complex to quench the free radicals was compared with that of quercetin (Q). The effect of time on the antioxidant activity of the samples was observed by addition of 0.01 M of the sample to DPPH solution and the absorbance values were recorded every five minutes up to 30 minutes. It is observed that the QGd complex exhibited higher scavenging ability than quercetin. The maximum DPPH scavenging activity for quercetin (~15%) was achieved within the first 5 min beyond which only a marginal increase was observed. QGd displayed a higher scavenging ability of about 23% within the first 5 minutes and continued to increase up to 25 minutes to reach a maximum of about 30% (Figure 6). A similar trend had been reported for several complexes

RSC Advances Accepted Manuscript

of Mn(II), Co(II), Ni(II), Cu(II) and Zn(II) [45]. The superior activity of the metal ion complexes had been attributed to their ability to stabilize the free radical. The results of the DPPH assay showing higher free radical scavenging activity for QGd reinforce the inferences drawn from the cyclic voltammetry studies.

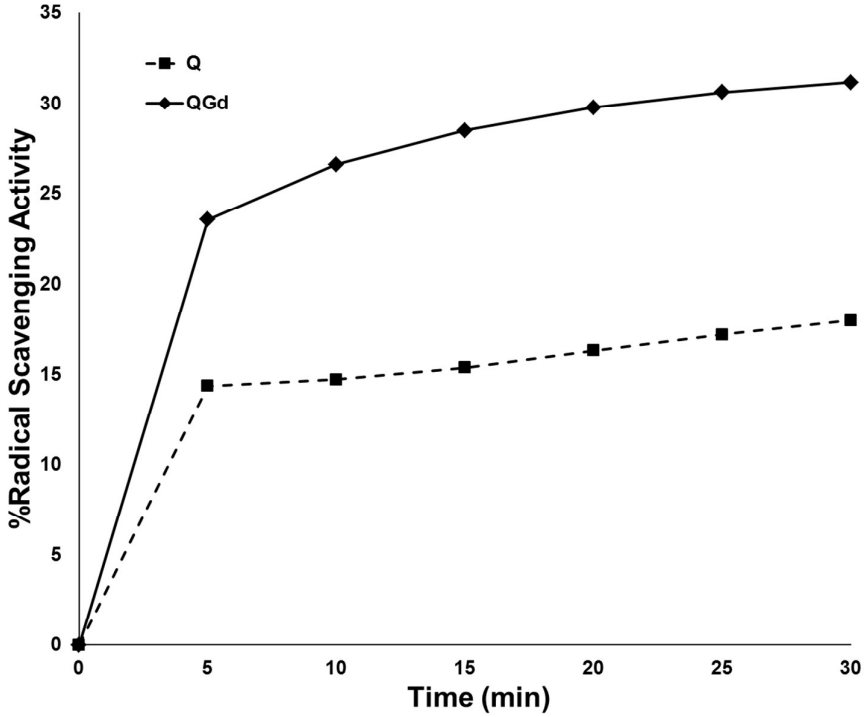

Figure 6. Scavenging activity of quercetin and quercetin-gadolinium (III) complex to DPPH radical

Cell viability (MTS assay) studies of Q and QGd complex

Figures 7A and 7B show the viability of L929 and MCF7 cells incubated with different concentrations of the samples. Interestingly, the viability of both L929 and MCF7 cells did not decrease even after 48h of exposure to the samples of concentrations up to 200 µg/mL. Quercetin has been shown by several groups to stimulate cell proliferation in MCF7 cells[56]. Our cytotoxicity data also correlates with this observation suggesting that quercetin does not exhibit toxic effects on MCF7 cells. It did not also affect the viability of normal cells suggesting its non-toxic nature. Gadolinium incorporated PEGylated silica particles have also

RSC Advances Accepted Manuscript

been reported to be non-toxic towards MCF7 cells[57]. Our data also suggests that Gadolinium acetate does not affect the viability of both cancer and normal cells. This may also be due to the poor permeability of free Gadolinium salt in to the cells resulting in the absence of any toxic effects. The QGd complex also did not adversely affect the viability of both normal as well as cancer cells. The absence of cytotoxicity augers well for its application as a magnetic contrast agent, as QGd is expected to cause no undesirable effects after administration.

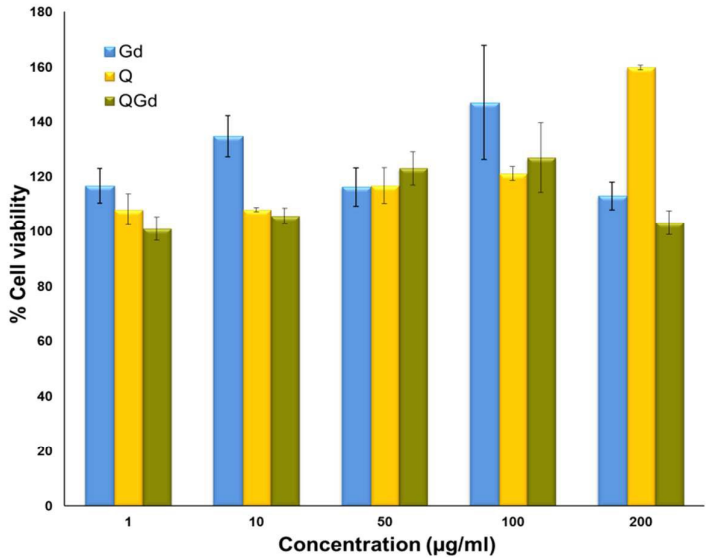

Figure 7A. Cell viability of MCF7 cells incubated for 48 h with gadolinium acetate hydrate(Gd), quercetin dihydrate(Q) and quercetin-gadolinium (III) (QGd)complex

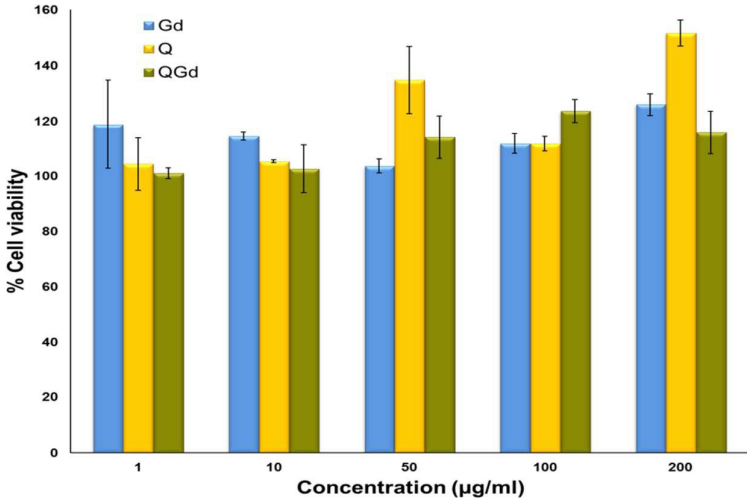

Figure 7B. Cell viability of L929 cells incubated for 48 h with gadolinium acetate hydrate(Gd), quercetin dihydrate(Q) and quercetin-gadolinium (III) (QGd)complex

RSC Advances Accepted Manuscript

MRI studies of QGd complex

An excited spin system on exposure to a magnetic field returns to its equilibrium magnetization through spin-lattice relaxation by transferring energy from the spin system to the lattice or the surroundings. The time taken for spin-lattice relaxation is referred to as the relaxation time T1 while the time taken for spin-spin relaxation is denoted as T2 [58]. Positive MRI contrast agents tend to decrease T1 relaxation times thereby increasing the magnitude of MR signal intensities [58]. Figure 8 shows the T1 weighted images of gadolinium acetate, quercetin-gadolinium complex and gadopentetate dimeglumine, a commercially available T1 contrast agent. It was found that all the three samples exhibit positive contrast. The MR signal intensity and T1 contrast tend to increase gradually as the concentration of the complex tends to increase from 10 to 500 µg/mL. Figure 9 shows the plot of longitudinal relaxation rate vs the concentration of the gadolinium acetate, quercetin-gadolinium complex and gadopentetate dimeglumine. A linear relationship was obtained for all samples and the values of r_1 and r_2 are summarized in Table 3. The relaxivities for gadolinium acetate, quercetin-gadolinium complex and gadopentetate dimeglumine are 0.0777, 0.2448 and 0.1934 $mM^{-1}s^{-1}$ respectively. Similarly transverse relaxation rates were calculated and the same trend was observed. The ratios of r_2/r_1 were found to be in the range of 1-3 indicating the positive contrast properties of the samples [59]. The gadolinium complexes are known for their T1 contrast behavior in MR imaging. However compared to gadolinium acetate, the contrast enhancement of quercetin-gadolinium complex was higher which is evident from the increase in r_1 value for the complex. The r_1 value of 0.2448 $mM^{-1}s^{-1}$ for quercetin-gadolinium complex is higher than the commercial T1 contrast agent gadopentetate dimeglumine with r_1 of 0.1934 $mM^{-1}s^{-1}$. The relaxivity r_1 is dependent on many factors including the molecular weight of the contrast agent [60]. One factor that may have contributed to the enhanced r_1 values for QGd may be its lower molecular weight when compared to gadolinium dimeglumine. The r_2 values

RSC Advances Accepted Manuscript

were also highest for QGd indicating that the complex could be employed for perfusion studies as a susceptibility agent [17].

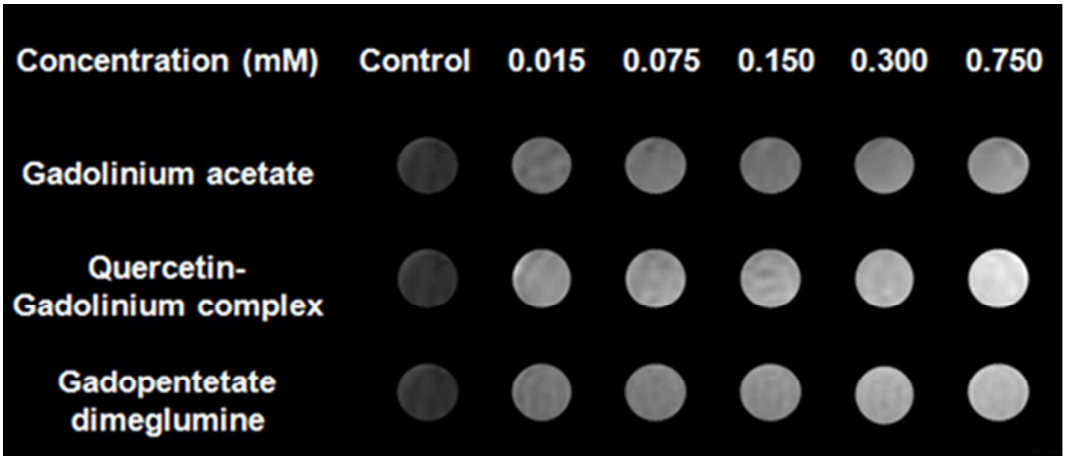

Figure 8. MRI image for Phantom agar gel assay of gadolinium acetate hydrate, quercetin-gadolinium complex and gadopentetate dimeglumine

Table 3. Relaxivity values of gadolinium acetate, quercetin-gadolinium complex and gadopentetate dimeglumine

Sample	r1	r2	r2/r1
Gadolinium acetate	0.0777	0.0859	1.1055
Quercetin-gadolinium complex	0.2448	0.6446	2.6331
Gadopentetate dimeglumine	0.1934	0.5922	3.0620

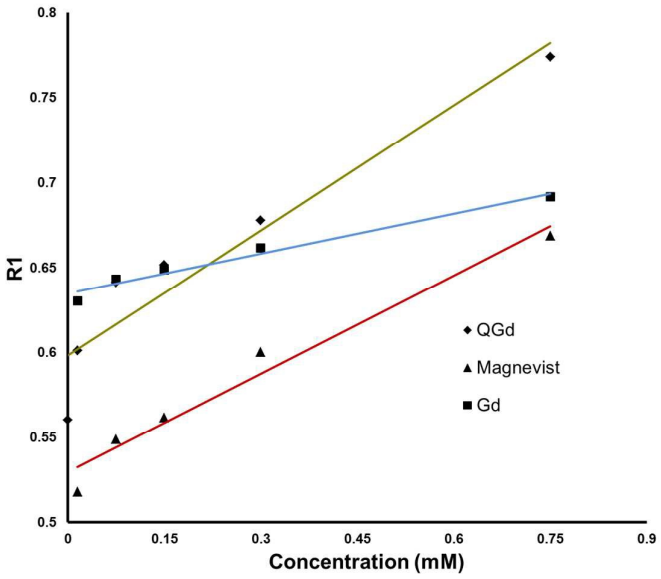

Figure 9. Comparison of relaxivity values for gadolinium acetate, quercetin-gadolinium complex and gadopentetate dimeglumine

RSC Advances Accepted Manuscript

***In vitro* MRI studies:** The contrast between the cells is known to increase with differences in T1 relaxation times between them. However, the inherent difference in T1 relaxation times between the pathologic and normal tissue is found to be insufficient to show a detectable contrast in the MR image. Hence use of appropriate contrast agents to enhance the contrast between the pathologic and normal tissues is essential. To evaluate the contrast properties of the quercetin-gadolinium complex, *in vitro* MR studies were performed at different time points for both cancer and normal cells (Table 4). The uptake of the complex by the cells was evaluated by measuring the relaxivity values and relaxation rates in MRI [61]. The *in vitro* MR studies for quercetin-gadolinium complex treated MCF7 cells and L929 cells exhibited significant difference in the intensity of positive contrast when compared with the untreated control cells (Figures 10A and 10B). It was found that the relaxivity (r_1 and r_2) of the complex in MCF7 cells was higher at the initial time point and gradually exhibited a progressive decrease with time. The r_2/r_1 ratios obtained for the MCF7 cancer cells incubated with QGd exhibit a progressive decrease with time but remain between 2 to 3 indicating positive contrast enhancement. However, the L929 cells exhibit an inverse trend with the r_1 relaxivity increasing from 3 h to 24 h. The r_2/r_1 ratios vary between 1.3 and 3.7 that lie in the typical range of positive contrast agents. The difference in the contrast enhancement with time between normal and cancer cells by QGd may be primarily attributed to the difference in their uptake and retention, since cancer cells generally have enhanced permeation when compared to normal cells [61]. This difference may be responsible for the higher relaxivity of cancer cells after 3 h when compared to their normal counterparts. The reduction in the contrast enhancement suggests the efflux of the contrast agent from the cancer cells. The normal cells, in comparison, exhibit a slower uptake that is manifested from the r_1 values. The results of the *in vitro* MRI demonstrate the feasibility of the use of QGd for cell tissue imaging applications to produce a strong MRI contrast.

RSC Advances Accepted Manuscript

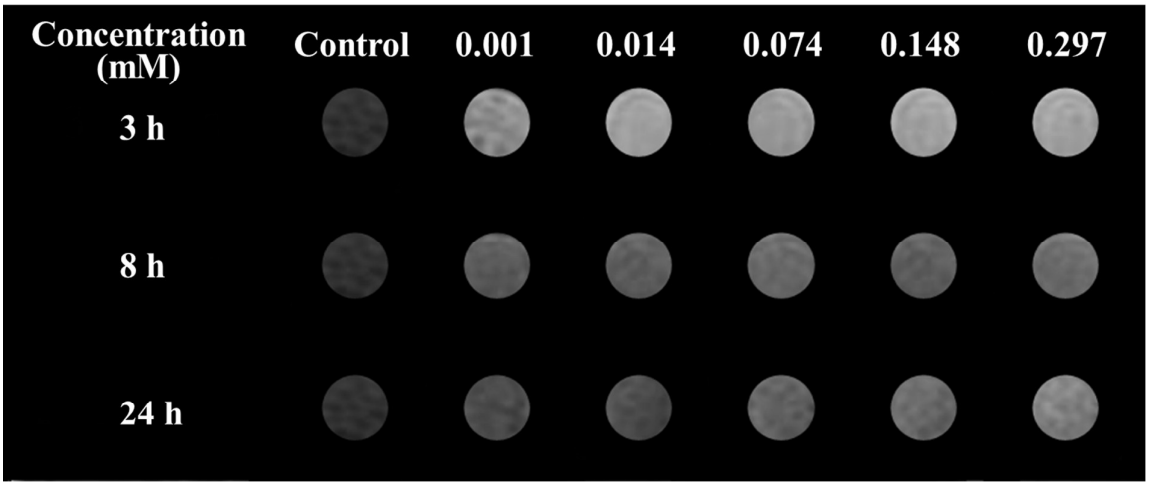

Figure 10A. MRI image for quercetin-gadolinium complex treated MCF7 cells

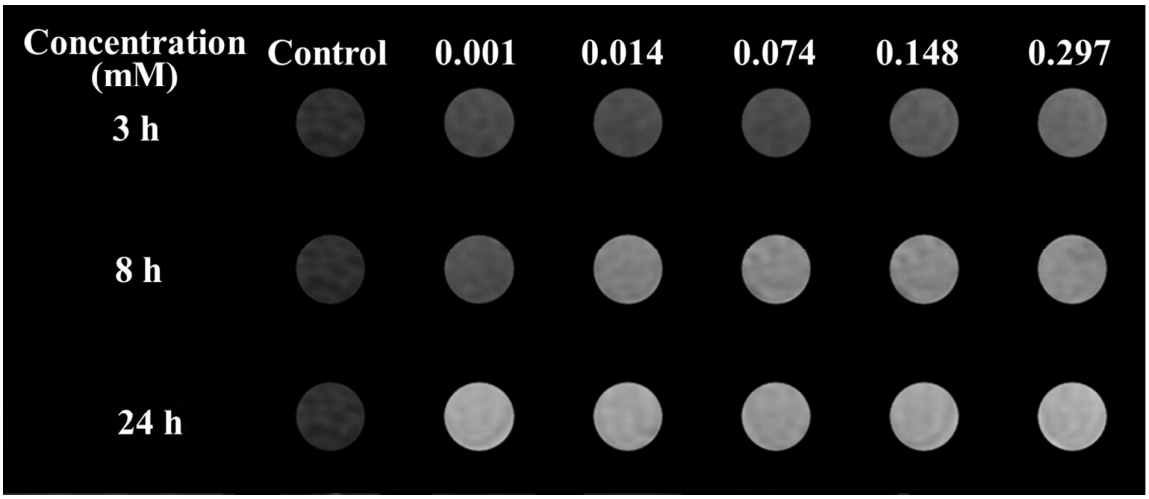

Figure 10B. MRI image for quercetin-gadolinium complex treated L929 cells

RSC Advances Accepted Manuscript

Table 4. *In vitro* MR imaging studies in MCF7 cells and L929 cells

Sample	Time (h)	r1	r2	r2/r1
MCF7	3	0.2285	0.6793	2.9728
	8	0.1887	0.3951	2.0938
	24	0.1755	0.3605	2.0541
L929	3	0.1921	0.6393	3.3279
	8	0.1859	0.6869	3.6949
	24	0.2361	0.3090	1.3087

Conclusion

Though lanthanide-flavonoid complexes have been reported in literature, their applications have been largely limited to anti-microbial and anti-cancer studies. This study for the first time explores the use of a flavonoid-lanthanide complex as a magnetic contrast enhancer. The present work successfully demonstrates the synthesis and characterization of a quercetin-gadolinium complex. The metal:ligand ratio was found to be 1:1 which was confirmed by different spectroscopic techniques and elemental analysis. The complex exhibited superior contrast properties when compared to the commercially used gadopentate dimeglumine. The *in vitro* MR contrast enhancement by the complex was demonstrated in both normal as well as cancer cells and the uptake variations between the cells were reflected in the relaxivity values. The quercetin-gadolinium complex did not affect the viability of both normal as well as cancer cells thus opening up new vistas for exploring this promising molecule for further pre-clinical and clinical trials as a magnetic contrast agent.

RSC Advances Accepted Manuscript

Acknowledgement

First author acknowledges the financial support from SASTRA University, Thanjavur - 613 401, India, under Prof. T. R. Rajagopalan research fund. All the authors acknowledge FIST, DST, India (SR/FST/LSI-327/2007 & SR/FST/LSI-453/2010) and SASTRA University for the infrastructural support.

References

1 J. P. Cornard, L. Dangleterre and C. Lapouge, *J. Phys. Chem. A*, 2005, **109**, 10044–51.

2 A. K. Verma, J. A. Johnson, M. N. Gould and M. A. Tanner, *Cancer Res.*, 1988, **48**, 5754–5758.

3 E. Middleton, C. Kandaswami and T. C. Theoharides, *Pharmacol. Rev.*, 2000, **52**, 673–751.

4 S. Birjees Bukhari, S. Memon, M. Mahroof Tahir and M. I. Bhanger, *J. Mol. Struct.*, 2008, **892**, 39–46.

5 Q. K. Panhwar, S. Memon and M. I. Bhanger, *J. Mol. Struct.*, 2010, **967**, 47–53.

6 W. Chen, S. Sun, W. cao, Y. Liang and J. Song, *J. Mol. Struct.*, 2009, **918**, 194–197.

7 N. Kawada, S. Seki, M. Inoue and T. Kuroki, *Hepatology*, 1998, **27**, 1265–1274.

8 P. C. Hollman, J. H. de Vries, S. D. van Leeuwen, M. J. Mengelers and M. B. Katan, *Am. J. Clin. Nutr.*, 1995, **62**, 1276–82.

9 P. C. H. Hollman, M. V. D. Gaag, M. J. B. Mengelers, J. M. P. Van Trijp, J. H. M. De Vries and M. B. Katan, *Free Radic. Biol. Med.*, 1996, **21**, 703–707.

10 M. Yoshida, T. Sakai, N. Hosokawa, N. Marui, K. Matsumoto, A. Fujioka, H. Nishino and A. Aoike, *FEBS Lett.*, 1990, **260**, 10–13.

11 and B. H. Long, L.H., M.V. Clement, *Biochem. Biophys. Res. Commun.*, 2000, **273**, 50–53.

12 D. R. Ferry, *Clin. Cancer Res.*, 1996, **2**, 659–668.

13 A. Torreggiani, M. Tamba, A. Trinchero and S. Bonora, in *Journal of Molecular Structure*, 2005, vol. 744-747, pp. 759–766.

14 S. Sun, W. Chen, W. Cao, F. Zhang, J. Song and C. Tian, *J. Mol. Struct. THEOCHEM*, 2008, **860**, 40–44.

RSC Advances Accepted Manuscript

15 D. Malešev and V. Kuntić, *J. Serbian Chem. Soc.*, 2007, **72**, 921–939.

16 J. P. Cornard and J. C. Merlin, *J. Inorg. Biochem.*, 2002, **92**, 19–27.

17 P. Caravan, J. J. Ellison, T. J. McMurry and R. B. Lauffer, *Chem. Rev.*, 1999, **99**, 2293–352.

18 P. Caravan, *Chem. Soc. Rev.*, 2006, **35**, 512–523.

19 P. H. Kuo, *Radiology*, 2004, **242**, 647–649.

20 F. Mostafaei, *Physiol. Meas.*, 2015, **36**, N1.

21 H. J. Weinmann, R. C. Brasch, W. R. Press and G. E. Wesbey, *Am. J. Roentgenol.*, 1984, **142**, 619–624.

22 M. Vorobiov, A. Basok, D. Tovbin, A. Shnaider, L. Katchko and B. Rogachev, *Nephrol. Dial. Transplant.*, 2003, **18**, 884–887.

23 N. Zlateva, G., Mileva, M. and Popdimitrova, in *Visible Photoluminescence of Solid State Quercetin and Rutin.*, 2007.

24 G. Dehghan and Z. Khoshkam, *Food Chem.*, 2012, **131**, 422–426.

25 G. M. and K. G. S. Pavia, D. L., Lampman, in *Introduction to spectroscopy(third edition)*, Brooks/Cole, A division of Thomson Learning, 2001.

26 S. Paul, N., Hazarika, *J. Appl. Phys.*, 2013, **114**, 134903.

27 C. E. Lekka, J. Ren, S. Meng and E. Kaxiras, *J. Phys. Chem. B*, 2009, **113**, 6478–6483.

28 S. Panhwar, Q.K. and Memon, *Pak J Anal Env. Chem*, 2012, **13**, 159–68.

29 S. Dowling, F. Regan and H. Hughes, *J. Inorg. Biochem.*, 2010, **104**, 1091–1098.

30 S. B. Bukhari, S. Memon, M. Mahroof-Tahir and M. I. Bhanger, *Spectrochim. Acta - Part A Mol. Biomol. Spectrosc.*, 2009, **71**, 1901–1906.

31 B. Steinbock, O., Neumann, *Anal. Chem.*, 1997, **69**, 3708–3713.

32 H. R. Weckhuysen, B., *Springer Berlin Heidelb.*, 2004, **4**, 295–335.

33 A. Bravo and J. R. Anacona, *Transit. Met. Chem.*, 2001, **26**, 20–23.

34 G. P. Guskos, N., riberis, *Phys. status solidi*, 1990, **162**, 243–249.

35 G. Zolnierkiewicz, *Rev. Adv. Mater. Sci,* 2006, **12**, 178–181.

36 Z. Dinya, I. Komáromi and A. Lévai, *J. Electron Spectros. Relat. Phenomena*, 1992, **59**, 315–325.

RSC Advances Accepted Manuscript

37 R. Tamrakar, *Adv. Phys. Lett.*, 2014, **1**, 1–5.

38 J. S. Renny, L. L. Tomasevich, E. H. Tallmadge and D. B. Collum, *Angew. Chemie - Int. Ed.*, 2013, **52**, 11998–12013.

39 M. C. H. Lukesh, B., *ARKIVOC*, 2005, **iii**, 200–210.

40 F. Rasoulzadeh, D. Asgari, a Naseri and M. R. Rashidi, *Daru*, 2010, **18**, 179–84.

41 R. Kim, C., and Savizky, *Res. J. Pharm. Biol. Chem. Sci. RJPBCS*, 2013, **4**, 765–795.

42 B. D. Wang, Z. Y. Yang, Q. Wang, T. K. Cai and P. Crewdson, *Bioorganic Med. Chem.*, 2006, **14**, 1880–1888.

43 B. Mishra, A. Barik, K. I. Priyadarsini and H. Mohan, *J. Chem. Sci.*, 2005, **117**, 641–647.

44 Y. Ni, S. Du and S. Kokot, *Anal. Chim. Acta*, 2007, **584**, 19–27.

45 P. Kavitha and K. Laxma Reddy, *Arab. J. Chem.*, 2013.

46 G. S. Borghetti, J. P. Carini, S. B. Honorato, A. P. Ayala, J. C. F. Moreira and V. L. Bassani, *Thermochim. Acta*, 2012, **539**, 109–114.

47 B. E. Warren, *Second ed(Dover, New York.)*, 1990.

48 A. Boultif and D. Louër, *J. Appl. Crystallogr.*, 2004, **37**, 724–731.

49 K. Jin, G.-Z., Y. Yamagata, and Tomita, *Acta Crystallogr. Sect. C*, 1990, **46**, 310–313.

50 P. C. R. Soares-Santos, H. I. S. Nogueira, V. Félix, M. G. B. Drew, R. A. Sá Ferreira, L. D. Carlos and T. Trindade, *Chem. Mater.*, 2003, **15**, 100–108.

51 A. Figuerola, *Inorg. Chem.*, 2003, **42**, 641–649.

52 G. Azizian, *Nanoscale Res. Lett.*, 2012, **7**, 1–10.

53 D. Zielińska, L. Nagels and M. K. Piskuła, *Anal. Chim. Acta*, 2008, **617**, 22–31.

54 A. M. O. Brett and M. E. Ghica, *Electroanalysis*, 2003, **15**, 1745–1750.

55 A. M. O. Ghica, M.E. and Brett, *Electroanalysis*, 2005, **17**, 313–318.

56 W.-Y. Zheng, S.-P. Nie, W.-J. Li, X.-J. Hu and M.-Y. Xie, *Food Biosci.*, 2013, **2**, 15–23.

57 Y. Yoon, B.-I. Lee, K. S. Lee, H. Heo, J. H. Lee, S.-H. Byeon and I. S. Lee, *Chem. Commun. (Camb).*, 2010, **46**, 3654–3656.

58 D. Zhu, F. Liu, L. Ma, D. Liu and Z. Wang, *Int. J. Mol. Sci.*, 2013, **14**, 10591–10607.

RSC Advances Accepted Manuscript

59 N. Leela Raghava Jaidev, Dhiraj Vasanth Bhavsar, Uma Sharma and U. M. K. & S. S. R. Jagannathan, *J. Biomater. Sci.*, 2014, **25**, 1093–1109.

60 S. Dumas, V. Jacques, W.-C. Sun, J. S. Troughton, J. T. Welch, J. M. Chasse, H. Schmitt-Willich and P. Caravan, *Invest. Radiol.*, 2010, **45**, 600–612.

61 Bjørnerud, in *The Physics of Magnetic Resonance Imaging*, Uppsala, 2008, pp. oslo:1–180.

RSC Advances Accepted Manuscript